Analysis of NMDA-independent long-term potentiation induced at CA3–CA1 synapses in rat hippocampus *in vitro*

C. Stricker*†, A. I. Cowan*†, A.C. Field*‡ and S. J. Redman*

**Division of Neuroscience, John Curtin School of Medical Research, Australian National University, GPO Box 334, Canberra, ACT 0200, Australia, †Institute of Neuroinformatics, ETHZ/UniZH, Winterthurerstrasse 190, CH-8057 Zürich, Switzerland and ‡Therapeutic Goods Administration, Health Department, PO Box 100, Woden, ACT 2606, Australia*

(Received 19 January 1999; accepted after revision 9 August 1999)

1. Excitatory postsynaptic currents (EPSCs) were evoked at synapses formed by Schaffer collaterals/commissural (CA3) axons with CA1 pyramidal cells using the rat hippocampal slice preparation. Long-term potentiation (LTP) was induced at these synapses using a pairing protocol, with 50 μM D,L-APV present in the artificial cerebrospinal fluid (ACSF).

2. Quantal analysis of the amplitudes of the control and conditioned EPSCs showed that the enhancement of synaptic strength was due entirely to an increase in quantal content of the EPSC. No change occurred in the quantal current.

3. These results were compared with those obtained from a previous quantal analysis of LTP induced in normal ACSF, where both quantal current and quantal content increased. The results suggest that calcium entering via NMDA receptors initiates the signalling cascade that results in enhanced AMPA currents because it is adding to cytoplasmic calcium from other sources to reach a threshold for this signalling pathway, or because calcium entering via NMDA receptors specifically activates this signalling pathway.

The signalling pathways leading to the induction of long-term potentiation (LTP) have been incompletely identified. It is generally accepted that LTP is triggered by an increase in cytoplasmic calcium concentration when this is coupled with synaptic excitation (Bliss & Collingridge, 1993). Post-synaptic calcium concentration can be elevated by calcium entry through NMDA receptors, through voltage-dependent calcium channels (VDCCs) and by release from intracellular stores. The relative importance of these sources of calcium at spinous synapses on CA1 pyramidal neurones is disputed in two recent reports (Emptage *et al.* 1999; Yuste *et al.* 1999), and the latter report suggests that calcium-permeable AMPA or kainate receptors may sometimes be present. At CA1 excitatory synapses, it was initially believed that calcium entry via NMDA receptors was a necessary condition for LTP induction (Bliss & Collingridge, 1993). Subsequent experiments demonstrated conditions under which a form of LTP could be induced, when NMDA channels were blocked, either by using brief 200 Hz tetani (Grover & Teyler, 1990*b*; Grover, 1998) or by pairing stimulation with pulses of postsynaptic depolarisation (Kullmann *et al.* 1992). These experiments provided the opportunity to compare the changes that take place in the two forms of LTP (NMDA-dependent and -independent) using quantal analysis. In an earlier report on NMDA-dependent LTP at excitatory synapses in CA1 pyramidal cells (Stricker *et al.* 1996*b*), we showed that LTP induced by a pairing protocol was accompanied by an increase in quantal AMPA current, together with an increase in the quantal content of this current. In the present report we have used identical experimental and analytical techniques, with the exception that the NMDA receptors have been blocked using D,L-2-amino-5-phosphonovaleric acid (D,L-APV), to show that in this form of NMDA-independent LTP no change occurs in the quantal AMPA current. The increase in synaptic strength is due solely to an increase in the quantal content of the AMPA current. This clear difference in the two forms of LTP expression has allowed us to propose that the signalling cascade leading to enhancement of AMPA currents is either triggered specifically by the calcium entering via NMDA receptors, or is initiated at a higher threshold of calcium concentration than the signalling cascade that results in an enhancement of quantal content.

METHODS

Preparation of hippocampal slices

Wistar rats of both sexes and aged from 17 to 28 days were decapitated using a guillotine. This procedure was approved by the Animal Ethics Committee of the Australian National University. The brain was then removed rapidly and placed in ice-cold artificial cerebrospinal fluid (ACSF) containing (mM): NaCl, 124; KCl, 3; $NaHCO_3$, 26; NaH_2PO_4, 2·5; $CaCl_2$, 2·5; $MgSO_4$, 1·3; glucose, 10. This solution was gassed with 95% O_2–5% CO_2 to obtain a final pH of 7·4. The brain was hemisected, and the cut surface glued to the

stage of a vibratome (Campden Instruments, Loughborough, UK) with cyanoacrylic glue. The stage was surrounded with ice-cold, gassed ACSF, and slices were cut at a thickness of 400 μm. The overlying cortex was removed from transverse hippocampal sections, which were then placed in a holding chamber and incubated at 34 °C for 1 h in ACSF. They were then maintained at room temperature (20–22 °C) until they were placed in the recording chamber.

Electrophysiology

The slices were transferred to a recording chamber, where they were superfused with gassed ACSF containing 10 μM bicuculline (Sigma) and 50 μM D,L-APV (Sigma, Tocris) at 30 °C. A cutting tool was made which contained a 50 μm gap in a razor blade, and this was used to make a transverse cut across the entire CA1 field, leaving only a 50 μm tissue bridge in stratum radiatum between CA3 and the region in CA1 from which recordings were made. Whole-cell voltage clamp recordings were obtained from CA1 neurones using the 'blind' patch clamp technique. Pipettes (3–5 MΩ) contained (mM): caesium gluconate, 130; CsCl, 9·5; EGTA, 0·2; Tes, 10; ATP, 3; GTP, 0·3; $CaCl_2$, 0·08; $MgCl_2$, 3; pH adjusted to 7·3; osmolarity, 270 mosmol l^{-1}. EPSCs (absolute mean amplitude < 8 pA) were evoked at 1 Hz by low-intensity, constant current stimulation (5–20 μA) of stratum radiatum, with pulse widths of 50–100 μs. The stimulation electrodes were very fine-tipped tungsten, or NaCl-filled patch electrodes. These were placed in CA1–CA3 stratum radiatum on the distal side of the tissue bridge.

The position of the stimulating electrode was altered, and the stimulating current varied, until a stimulus–response relationship that contained a clear plateau region (such as that shown in Fig. 1*A* of Stricker *et al.* 1996*a*) was obtained. In this plateau region, the EPSC amplitude remained constant as the stimulus current was increased. Ideally, this range needed to be >10 μA. The stimulus current was then adjusted to the mid-range of the plateau region, and recordings were taken at 1 Hz for 600 control records. Conditioning of the EPSC to induce LTP involved pairing 2 Hz stimulation with depolarisation to 0 or +10 mV for 100–200 stimuli. Conditioned responses were then recorded for as long as stable recording conditions could be maintained. Access resistance was continuously monitored by recording the current response to a 0·5 mV depolarising voltage step of 40 ms duration on each recording trace. Individual records were filtered at 1 kHz using a 4-pole Bessel filter, digitised (12 bit) at 5 kHz and stored on computer.

Analysis

The first step in off-line analysis was to remove as much of the stimulus artifact from the baseline and rising phase regions of the EPSC as possible. This was done by averaging all records which clearly contained no EPSC (failures) and subtracting this mean from all records. The peak amplitude of the EPSC was then obtained by manually placing cursors in the baseline and peak regions for each record, averaging the current in each time window, and subtracting the baseline current from the peak current. The same procedure was used to obtain a measure of baseline noise. The details of window width, separation and placement are described fully in Stricker *et al.* (1996*a*).

The data were first checked for stationarity. Once periods were identified where the EPSC amplitude satisfied the criteria for stationarity, the peak EPSC, and the noise currents from these regions, were used to form probability density functions (p.d.f.s). This was done by convolving each current with a normal distribution having a mean of zero and a standard deviation that depended on the sample size, the standard deviation of the baseline noise and a preliminary estimate of the quantal current. The details have been provided in Stricker *et al.* (1996*a*).

The analysis procedures have been designed to allow a systematic evaluation of a hierarchy of possible statistical models of transmission, using a null hypothesis (H_0) for rejection or acceptance in each case. The null hypothesis test was based on the ability of each model to fit the measured p.d.f. using the maximum likelihood criterion. When the null hypothesis cannot be rejected, the model with the smaller number of parameters was accepted (principle of parsimony). First, an unconstrained mixture of normal distributions was tested against the null hypothesis that the p.d.f. was a unimodal distribution. If H_0 could be rejected, models of transmission with increasing numbers of constraints were tested against the less complex models (as H_0). The models considered were: (a) a quantal model where the normal distributions in the mixture model (above) are separated by a constant increment (the quantal amplitude Q); (b) a quantal model as in (a) but with quantal variance added to the noise variance; (c) a quantal model with binomial release probabilities, with or without quantal variance; (d) a quantal model with compound binomial release probabilities, with or without quantal variance.

Each of these models of transmission had their parameters adjusted to maximize the likelihood of the fit to the p.d.f. of the EPSC using the Expectation–Maximization (EM) algorithm. The formulae required were derived in Stricker & Redman (1994). Complete details on how competing models of transmission were evaluated were given in Stricker *et al.* (1994). Once the most appropriate model of transmission was determined, the quantal current, quantal content and quantal variance were extracted.

Correction for the distorting effects of access resistance

The access resistance was determined from the current response to a 0·5 mV depolarising step, as described in Stricker *et al.* (1996*a*). The clamp error in the synaptic current caused by access resistance was then estimated, using a compartmental model of a CA1 pyramidal cell, the time course and amplitude of the synaptic current, the input resistance of the cell under investigation and the measured access resistance. The imperfect clamp was simulated, and then with access resistance made zero, the undistorted synaptic current time course and amplitude were calculated. This correction allowed a comparison of quantal currents between different experiments. More details are given in Stricker *et al.* (1996*a*).

RESULTS

The results are based on a complete statistical analysis of seven EPSCs for which stable LTP was recorded for a minimum of 19 min. Data obtained from a further 18 EPSCs have not been used for several reasons. Four EPSCs were excluded for technical reasons; a large change in access resistance occurred during recording of the conditioned EPSC (2 experiments) and the recording of the conditioned EPSC was lost before a sufficient number of EPSCs had been obtained (2 experiments). Eight EPSCs were not considered because the LTP was not maintained for at least 19 min (3 EPSCs) or the EPSC depressed following conditioning (5 EPSCs). Possible reasons for failure to induce maintained LTP are given in the Discussion. For the remaining 6 EPSCs, LTP was maintained for longer than 20 min, but the p.d.f. of the peak amplitudes for either the control or the

Table 1

Cell no.		N	t (min)	σ_n (pA)	Mean (pA)	LTP (%)	R_A (MΩ)	R_I (MΩ)	T_R (ms)	T_{HW} (ms)	Scale	Dist (λ)	Model	K	Q (pA)	c.v.	m	P_0
1	C	572	−10	0·97	−13·8±11·3	0	12	115	2·1	7·8	1·7	0·4	UQv	13	−5·3±0·1	0·08±0·04	4·5±0·2	0·14±0·01
	P	1008	53	1·05	−15·6±11·7	14±3	12	92	2·0	8·1	1·8	0·4	UQv	14	−5·2±0·1	0·18±0·07	5·3±0·2	0·37±0·02
2	C	320	−17	0·6	−5·4±4·1	0	33	143	2·6	17·4	2·8	0·4	BQv	6	−10·3±0·5	0·35±0·05	1·5±0·1	0·21±0·02
	P	714	15	0·8	−19·1±7·1	232±5	32	108	2·9	21·4	2·6	0·6	UQv	10	−9·3±0·4	0·17±0·07	5·3±0·3	0·0
	P	970	56	0·7	−15·6±7·6	144±4	29	106	3·6	16·2	2·4	0·6	UQv	10	−8·0±0·3	0·22±0·04	4·6±0·2	0·0
3	C	560	−12	0·9	−7·4±7·2	0	17	151	2·4	10·3	2·0	0·3	UQv	6	−8·7±0·2	0·17±0·03	1·7±0·1	0·37±0·02
	P	500	20	0·9	−13·3±7·4	89±4	19	119	2·2	9·3	2·1	0·3	UQv	6	−8·6±0·7	0·41±0·05	3·3±0·3	0·06±0·01
4	C	653	−13	0·6	−7·3±5·6	0	29	140	3·5	13·6	2·4	0·5	UQ	10	−5·5±0·5	—	3·2±0·3	0·22±0·02
	P	520	53	0·6	−11·7±5·9	113±3	41	142	3·2	11·8	3·2	0·4	UQv	14	−5·7±0·1	0·10±0·02	6·6±0·2	0·02±0·01
5	C	533	−10	0·6	−1·7±2·8	0	22	165	2·9	13·5	2·1	0·4	UQ	5	−5·3±0·5	—	0·7±0·1	0·70±0·02
	P	614	19	0·7	−3·6±3·5	82±7	17	134	3·0	15·2	1·9	0·5	UQ	6	−4·5±0·2	—	1·5±0·1	0·38±0·02
6	C	504	−10	0·8	−2·0±2·0	0	18	116	2·2	13·9	2·1	0·4	UQ	4	−5·1±0·2	—	0·8±0·1	0·51±0·03
	P	1030	38	0·8	−6·5±7·6	199±8	17	106	2·6	12·0	2·0	0·5	UQ	13	−4·7±0·4	—	2·7±0·2	0·33±0·02
	P	1620	68	0·8	−8·8±10·8	222±9	11	96	2·8	11·7	1·6	0·6	UQv	17	−4·0±0·1	0·10±0·03	3·4±0·1	0·30±0·01
7	C	760	−13	0·6	−5·7±4·3	0	9	131	2·4	12·3	1·5	0·4	UQv	6	−4·2±0·1	0·15±0·01	2·0±0·1	0·21±0·01
	P	708	20	0·8	−11·3±7·0	85±5	8	124	3·4	16·7	1·4	0·7	UQv	9	−4·4±0·1	0·14±0·02	3·5±0·1	0·08±0·02

Where applicable the values are given in means ± s.d. C corresponds to control records; P to potentiated records. N, number of records used to construct p.d.f. t, time in minutes over which recording was maintained. σ_n, standard deviation of noise. Mean, mean amplitude of EPSC. LTP, percentage increase in EPSC following conditioning. Zero indicates no change. R_A, access resistance. R_I, input resistance of neurone. T_R, 10–90% rise time of EPSC. T_{HW}, half-width of EPSC. Scale, scaling factor to apply to measured amplitudes to compensate for the effect of access resistance. Dist, electrotonic distance from soma to where the weighted mean EPSC originates. Model, type of model that best fits the p.d.f.: UQ, unconstrained quantal model; UQv, unconstrained quantal model with variance; BQv, binomial quantal model with quantal variance. K, number of detectable release sites. Q, quantal AMPA current. c.v., coefficient of variation of quantal current; — indicates no quantal variance was required. m, quantal content. P_0, probability of failures.

conditioned EPSC did not satisfy our statistical criteria for quantisation. This is a higher success rate for quantisation (7/13) than that reported in a previous investigation (19/50) on quantal analysis of CA1 EPSCs (Stricker *et al.* 1996*a*).

An example of successful conditioning of an EPSC is shown in Fig. 1*A*, where each dot is the peak amplitude of the EPSC evoked at 1 Hz. The first conditioning stimulus (2 Hz for 200 stimuli paired with 0 mV depolarisation – first bar on time axis) did not enhance the EPSC. A second conditioning stimulus (2 Hz for 200 stimuli at +10 mV – second bar on time axis) caused the EPSC to be potentiated and this was maintained for the duration over which stable recording conditions could be maintained (68 min). LTP was maintained for more than 50 min for four EPSCs (see Table 1). The pooled means of the normalised amount of NMDA-independent potentiation for all EPSCs for the first 45 min following induction are shown in Fig. 1*B*. The mean potentiation over the first 45 min is 73 ± 14%. The graph above the pooled means indicates the number of experiments included in the mean at any time. The increase in the error bars towards the end of the pooled means reflects the smaller number of recordings obtained for longer durations. Not all recordings were sufficiently stationary throughout their time course for reliable statistical analysis. Shorter periods of continuous recording which were sufficiently stationary were selected for quantal analysis, and the number of records used (N) is indicated in Table 1. The mean potentiation over the periods of stationarity was 116 ± 28% (mean ± s.d.; $n = 7$) compared with 198 ± 37% ($n = 11$) for NMDA-dependent LTP (Stricker *et al.* 1996*b*). This difference is close to being statistically significant (Student's t test, $P = 0{\cdot}07$). For all EPSCs, cessation of recording was caused by loss of stable recording conditions and not by run-down of LTP.

The results from two control experiments supported the reliability of the result in Fig. 1*B*. In the first (Fig. 2*A*), no conditioning stimulation was applied, and the recordings were maintained for similar durations to those achieved for Fig. 1*B*. If the excitation threshold of axons excited by the extracellular stimulus altered over time, it would cause drift in the EPSC amplitude. No such drift was observed. In the second control experiment (Fig. 2*B*), the neurone was depolarised to 0 mV for 120 s following a period of control recording, but with the stimulator off. Stimulation was then

resumed. The EPSCs initially potentiated following the depolarisation (inset), and then depressed in all recordings ($n = 5$).

To ensure that all NMDA receptor current was blocked under our experimental conditions by 50 μM D,L-APV, the evoked EPSC was first recorded in normal ACSF at a membrane potential of −30 mV. This measurement was then repeated with 5–10 μM 6,7-dinitro-quinoxaline-2,3-dione (DNQX) in the ACSF, and following the further addition of 50 μM D,L-APV (Fig. 3*A*). Under the last condition, a complete block of transmission was always present ($n = 8$ at 1 Hz), indicating the effectiveness of this concentration of APV. The amplitudes of the EPSCs used in these experiments were bigger than those documented in Table 1 to increase released glutamate and to make any residual EPSC more detectable. Furthermore, we investigated the block of the NMDA receptors at different frequencies of stimulation (Fig. 3*B*) to examine the completeness of the NMDA receptor block during increased glutamate release at higher stimulation frequencies. The mean EPSCs were obtained from 200 stimuli at varying frequencies (1–20 Hz) while holding the membrane potential at −30 mV in order to achieve sufficient driving force for the synaptic current. At stimulation frequencies equal to 5 Hz, there was no detectable current (< 3 %). At higher frequencies, there was a small remaining current in one out of four experiments (< 10 %; $P = 0{\cdot}05$, Student's t test) and a similar tendency in one other experiment ($P = 0{\cdot}1$, t test). Thus, at the stimulation frequency used during the conditioning protocol (2 Hz), there was no evidence for an incomplete block of the NMDA receptors.

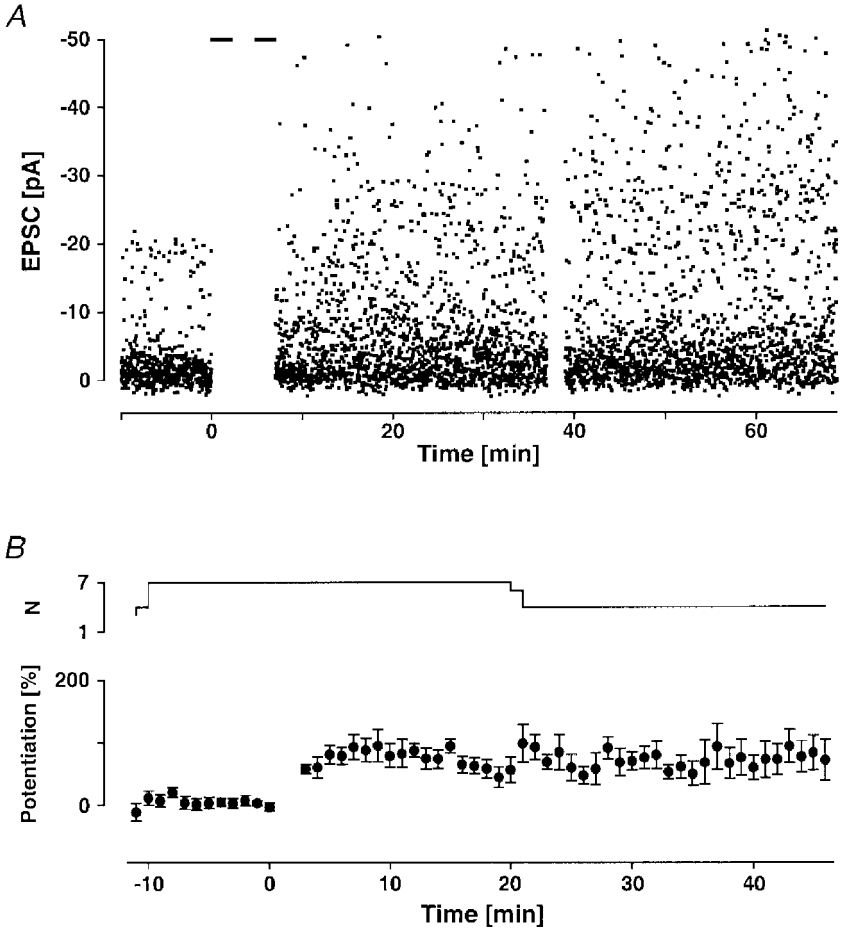

Figure 1

A, the EPSC (Cell 6) was evoked at 1 Hz for 10 min. Depolarisation to 0 mV was coupled with 2 Hz stimulation for 200 stimuli at time zero (first time bar). The EPSC was then recorded for 220 responses (amplitude measurements not shown), when it became clear that there was no potentiation. During the second time bar, depolarisation to +10 mV was paired with 2 Hz stimulation for 200 stimuli and the EPSC potentiated. The gap at 38 min occurred when a second conditioned data file was set up. Each dot represents the peak amplitude of a single EPSC. *B*, pooled and normalised means of EPSCs over time for all 7 results. Each point corresponds to the mean amplitude ± S.E.M. for 60 successive responses. Zero time corresponds to the start of the conditioning period. The line above the graph indicates how many recordings could be included to generate the pooled mean. The error bars are bigger towards the tail of the pooled means because a smaller number of recordings were included.

The peak amplitudes of the control and potentiated responses in APV were used to make p.d.f.s (Stricker *et al.* 1996*a*). Continuous periods of recording during which the EPSC amplitude remained stationary were selected for this analysis. The number of records used for each p.d.f. is indicated by N (in Table 1). This was often less than the total number of EPSCs recorded. The p.d.f.s for one set of EPSCs are shown in Fig. 4*A* and *C* (Cell 7, Table 1) as thick lines. Both p.d.f.s easily pass the test for reliable quantisation (described in Stricker *et al.* 1996*a*). The optimal statistical description for the control p.d.f. is a quantal process, with a quantal current of $2{\cdot}9 \pm 0{\cdot}04$ pA (mean ± s.d.), a coefficient of variation (c.v.) of $0{\cdot}15 \pm 0{\cdot}01$, and with a minimum of 6 discrete amplitudes (including failures) contributing to the EPSC. These amplitudes and their probabilities are shown in Fig. 4*B*, and the p.d.f. corresponding to this statistical description is the thin line superimposed on the data (thick line) in Fig. 4*A*. The probabilities associated with the discrete amplitudes could not be described by a binomial process. Following conditioning, the mean EPSC over the next 16 min was $11{\cdot}3 \pm 7{\cdot}0$ pA (compared with $5{\cdot}7 \pm 4{\cdot}3$ pA during the control recording). The p.d.f. of the conditioned responses is shown in Fig. 4*C*. Again, the optimal statistical description for this p.d.f. is that of a quantal process, with no classical description possible for the probabilities attached to each discrete amplitude. The quantal current is $3{\cdot}2 \pm 0{\cdot}1$ pA, the c.v. of the quantal current is $0{\cdot}14 \pm 0{\cdot}02$, and the minimum number of discrete amplitudes is 9. These amplitudes, their probabilities, and the error bars associated with them are shown in Fig. 4*D*. Full details are available in Table 1 (Cell 7).

A similar analysis was performed on the other six EPSCs. All the details of these analyses are provided in Table 1. Four control EPSCs required quantal variance in their statistical characterization, while six conditioned EPSCs required quantal variance. Only one EPSC (Cell 2) could have its release process described by a binomial process, and then only for the control responses. For all EPSCs, conditioning resulted in an increased quantal content and no increase in quantal current. The probability of failure decreased for all EPSCs except one (Cell 1). These results are summarized in Fig. 5*A*, where the quantal current before and after conditioning is shown, and similarly for the quantal content (Fig. 5*C*). The quantal currents in Fig. 5*A* are different from those calculated from the p.d.f.s as they have been corrected for the effects of access resistance

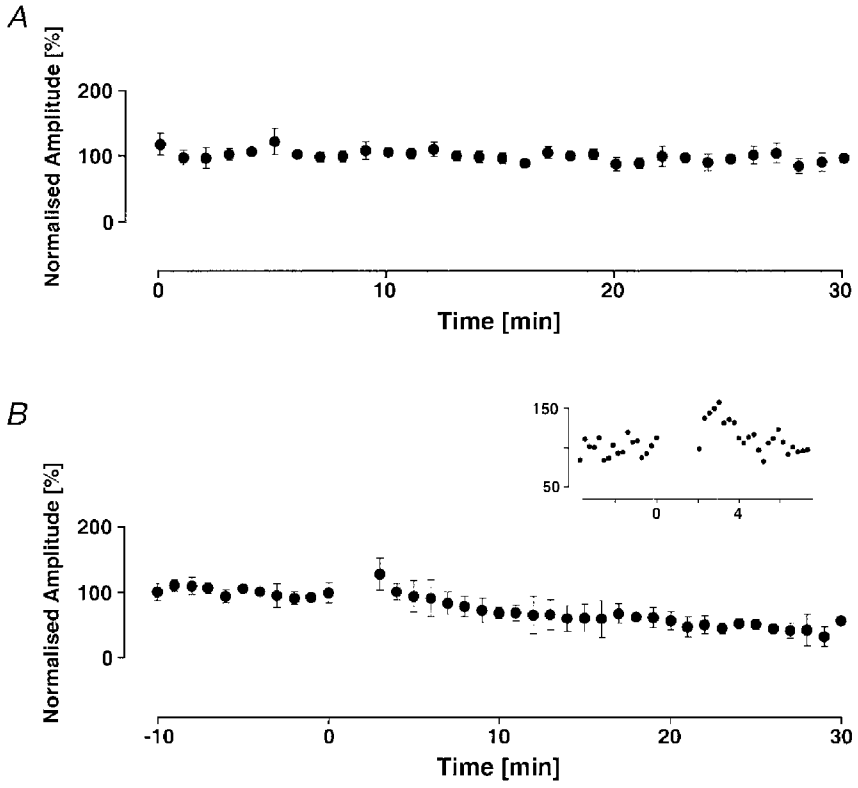

Figure 2. Control experiments

Each point is the mean of 60 evoked EPSCs (1 min). *A*, normalised peak amplitudes at 1 Hz stimulation during a control period of 30 min. The mean peak amplitude of the underlying EPSCs is $-5{\cdot}7 \pm 2{\cdot}3$ pA (5 experiments) This stable response was significantly different from the potentiated response in Fig. 1*B*. ($\chi^2_1 = 5{\cdot}0$; $P < 0{\cdot}05$). *B*, after a baseline recording period of 10 min the postsynaptic cell was clamped to 0 mV for 120 s with no stimulation of the presynaptic fibres. Subsequently, the synaptic currents depressed in all experiments ($n = 5$; $P < 0{\cdot}05$). The inset illustrates a transient potentiation immediately following the depolarisation, which lasted for about 2 min. This transient potentiation was present in all 5 recordings.

(Stricker *et al.* 1996*a*). The access resistances, and the scaling factors to apply to each EPSC if the access resistance had been zero are given in Table 1. It is clear from Fig. 5*A* and *B* that the quantal current was unchanged by conditioning for all 7 EPSCs, while the quantal content increased for all EPSCs. It follows that the amount of potentiation is proportional to the percentage increase in quantal content (Fig. 5*D*), and does not involve any change in quantal current (Fig. 5*B*).

The increase in quantal content indicates that more sites are involved in transmission, because transmission occurs at previously silent sites and/or the probability of transmitter release has increased at previously active sites. This change could be reflected in a change in the mean synaptic locus for generation of the composite EPSC. The mean synaptic location on the dendritic tree was calculated for all EPSCs. This was done by simulating the imperfect voltage clamp, as described in Methods. An AMPA conductance change was placed at different locations on the dendritic tree of the compartmental neurone until the recorded time course of the EPSC matched the simulated time course (further details were given in Stricker *et al.* 1996*a*). This calculation was made for both the control and conditioned EPSCs, using the input resistance and access resistance that pertained to those recordings. While it is a simplification to suggest that the synaptic contacts activated by minimal stimulation will all be at similar dendritic locations, this calculation gives a location equivalent to a weighted mean location of the distributed synaptic inputs. Table 1 gives this synaptic location on the apical dendrite (in electrotonic distance), as

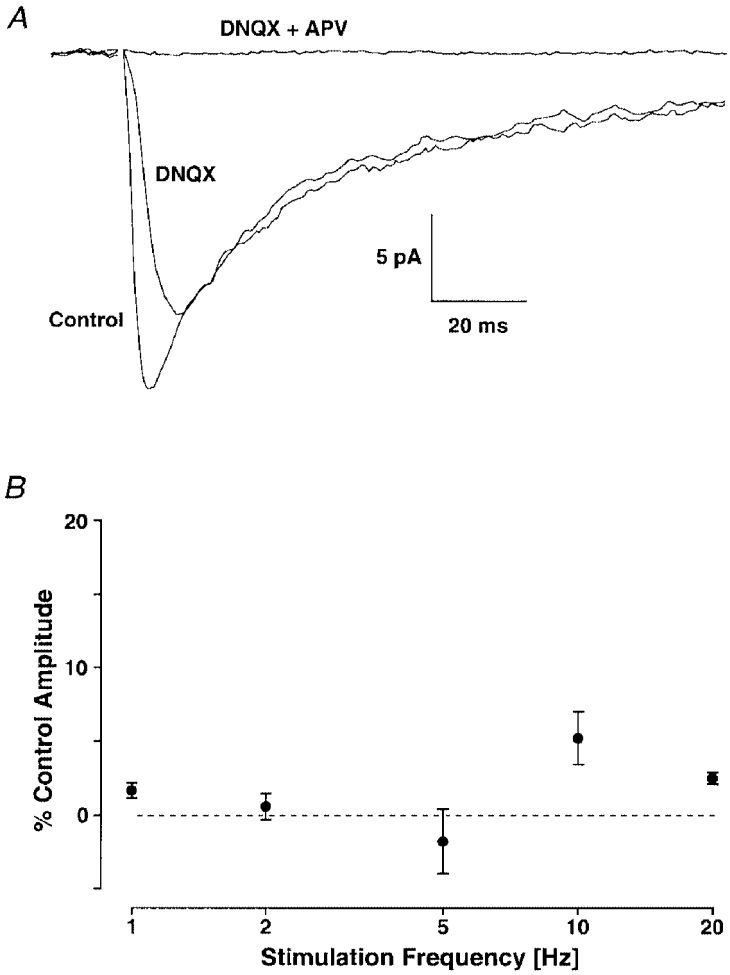

Figure 3. Block of the EPSC by 50 μM D,L-APV

A, to simulate the conditions of the pairing procedure, the EPSCs were obtained from 200 stimuli at 2 Hz while holding the membrane potential at −30 mV. For clarity the size of the underlying EPSC was chosen to be about 3 times bigger than those documented in Table 1. The faster AMPA receptor component was blocked by the addition of 5 μM DNQX, leaving a slowly rising prolonged NMDA receptor-mediated EPSC. The addition of 50 μM D,L-APV completely abolished the remaining EPSC. *B*, block of the NMDA EPSC at varying stimulation frequencies ($n = 4$). The EPSC recorded in APV was normalised with respect to the amplitude recorded in the absence of APV and plotted against the stimulation frequency (logarithmic scale). The error bars indicate S.E.M. Note that at frequencies up to 5 Hz, the block of the peak NMDA current amplitude is not different from zero (Student's *t* test). The dashed line indicates full block of the underlying NMDA current.

well at the rise time and half-width of the EPSC corrected for the distortion caused by the access resistance.

The synaptic location was increased following conditioning for four EPSCs, showed little change for two EPSCs, and decreased for the remaining EPSC. Changes in synaptic location are consistent with increases in quantal content, for the reasons mentioned above. A similar result was obtained for LTP in normal ACSF (Stricker *et al.* 1996*b*, their Fig. 6).

DISCUSSION

An important advance in understanding mechanisms of LTP in the mammalian brain came with the discovery that the induction of LTP at synapses formed by Schaffer collaterals with CA1 pyramidal neurones was dependent on NMDA receptor activation (Collingridge *et al.* 1983). Subsequent experiments have shown that by using more robust induction protocols than those generally used to induce NMDA-dependent LTP, NMDA-independent forms of LTP can be demonstrated at these synapses (Grover & Teyler, 1990*a*; Kullmann *et al.* 1992; Grover, 1998). The implication was that the calcium required to trigger LTP induction could be obtained from voltage-dependent calcium channels and/or from intracellular stores. The induction protocols were 200 Hz tetani (Grover & Teyler, 1990*b*) or long depolarising pulses to 0 mV paired with 120–200 stimuli at 2 Hz (Kullmann *et al.* 1992). In the present experiment, it was necessary to give 200 stimuli at 2 Hz, and sometimes repeat this while maintaining the membrane potential of the soma at 0 mV, i.e. at least twice the number of stimuli normally used to induce NMDA-dependent LTP by pairing depolarisation with 2 Hz stimulation (Stricker *et al.* 1996*b*).

Even with this more prolonged pairing protocol, the success rate for obtaining a maintained potentiation was low (at most 13/21) compared with the pulsed protocol combined with 4 mM Ca^{2+} in the ACSF used by Kullmann *et al.* (1992, see their Fig. 7). The probable explanation is that voltage pulses minimise calcium channel inactivation, and when

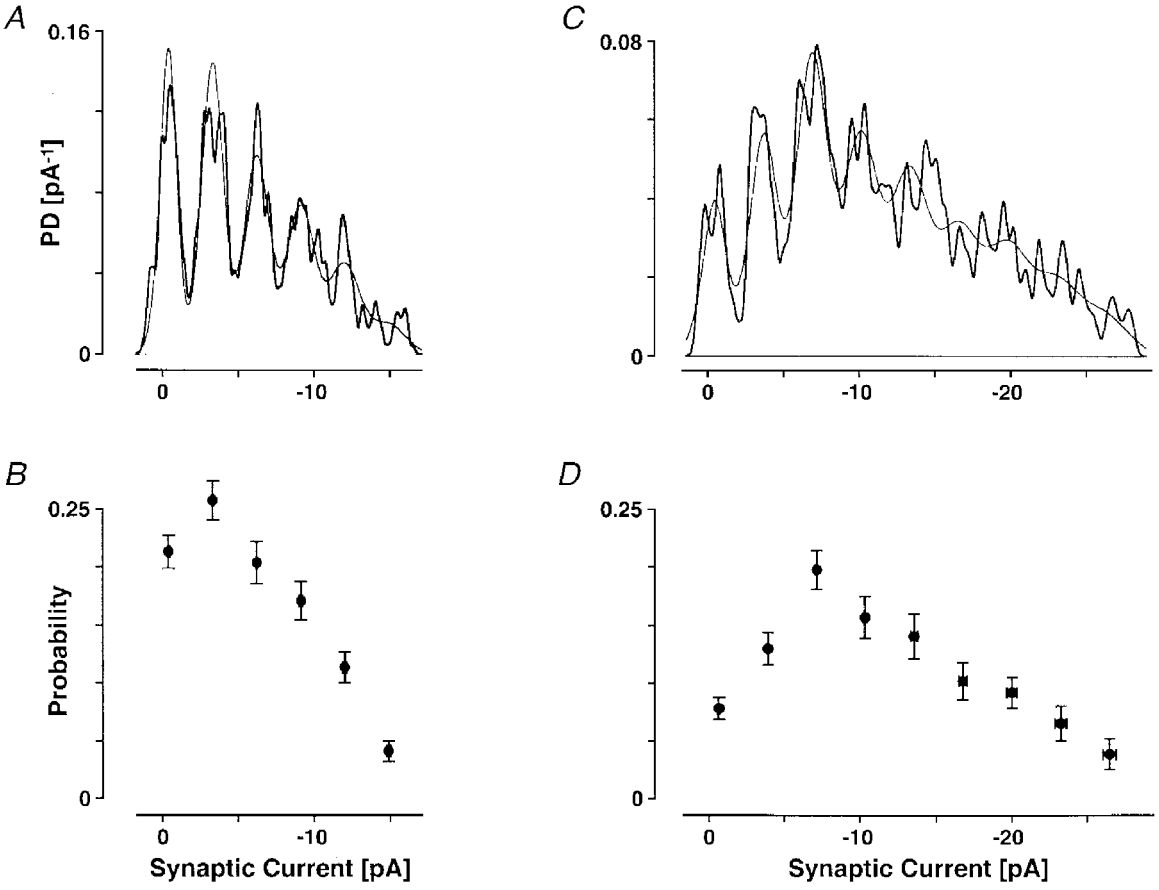

Figure 4

A, the thick line is the probability density function (p.d.f.) formed from the peak amplitudes of 760 control EPSCs using a Gaussian kernel ($\sigma = 0{\cdot}14$ pA). The noise standard deviation was 0·6 pA. The thin line is the optimal fit to this p.d.f.. This is a quantal model, with no constraints placed on the statistics of the release process and with a coefficient of variation (c.v.) of the quantal current equal to 0·15. Other details may be obtained from Table 1, entry Cell 7 C. *B*, the discrete amplitudes of the EPSCs, and their associated probabilities together with confidence limits for the probabilities. The confidence limits for the amplitudes are negligible. *C* and *D*, similar to *A* and *B*. The p.d.f. in *C* was formed from 708 EPSCs using a Gaussian kernel ($\sigma = 0{\cdot}20$ pA), which were obtained during the first 16 min after conditioning, when the EPSC means and variances per minute indicated a stationary process. All the details are given in Table 1, Cell 7 P.

combined with a much higher external calcium concentration, a greater calcium influx is achieved. Further evidence for the enhanced entry of calcium obtained with voltage pulsing can be found by comparing the result in Fig. 2*B* (conditioning without stimulation and with maintained depolarisation) with those in Fig. 1 of Kullmann *et al.* (1992) where the calcium-dependent transient potentiation that occurred following voltage pulsing alone was more enhanced and prolonged than in the present results. This transient potentiation was blocked by nifedipine, indicating that calcium entry through inactivating L-type channels is required for its induction (Kullmann *et al.* 1992). The fact that our conditioning protocol resulted in depression in 5/21 EPSCs is consistent with the notion that maintained depolarisation in the presence of APV does not guarantee adequate calcium entry for the reliable induction of LTP, and inadequate calcium results in depression.

When the results presented here are compared with those obtained for NMDA-dependent LTP (Stricker *et al.* 1996*b*), there are some clear differences. The two sets of results have been combined in Fig. 6. The mean of the percentage increase in quantal content, normalised by the percentage increase in the EPSC was $59 \pm 35\%$ ($n = 11$) for NMDA-dependent LTP and $104 \pm 8\%$ ($n = 7$) for NMDA-independent LTP. These results are significantly different ($P = 0{\cdot}004$, Student's t test). The mean of the percentage increase in quantal current, also normalised by the percentage increase in the EPSC, was $23 \pm 25\%$ ($n = 11$) for NMDA-dependent LTP and $-4 \pm 8\%$ ($n = 7$) for NMDA-independent LTP. This difference is also significant ($P = 0{\cdot}01$). Thus on a population basis, the two sets of results are clearly different. If we examine the difference between both sets of experiments only over the range of potentiation achieved with NMDA-independent LTP (14–232%), the percentage

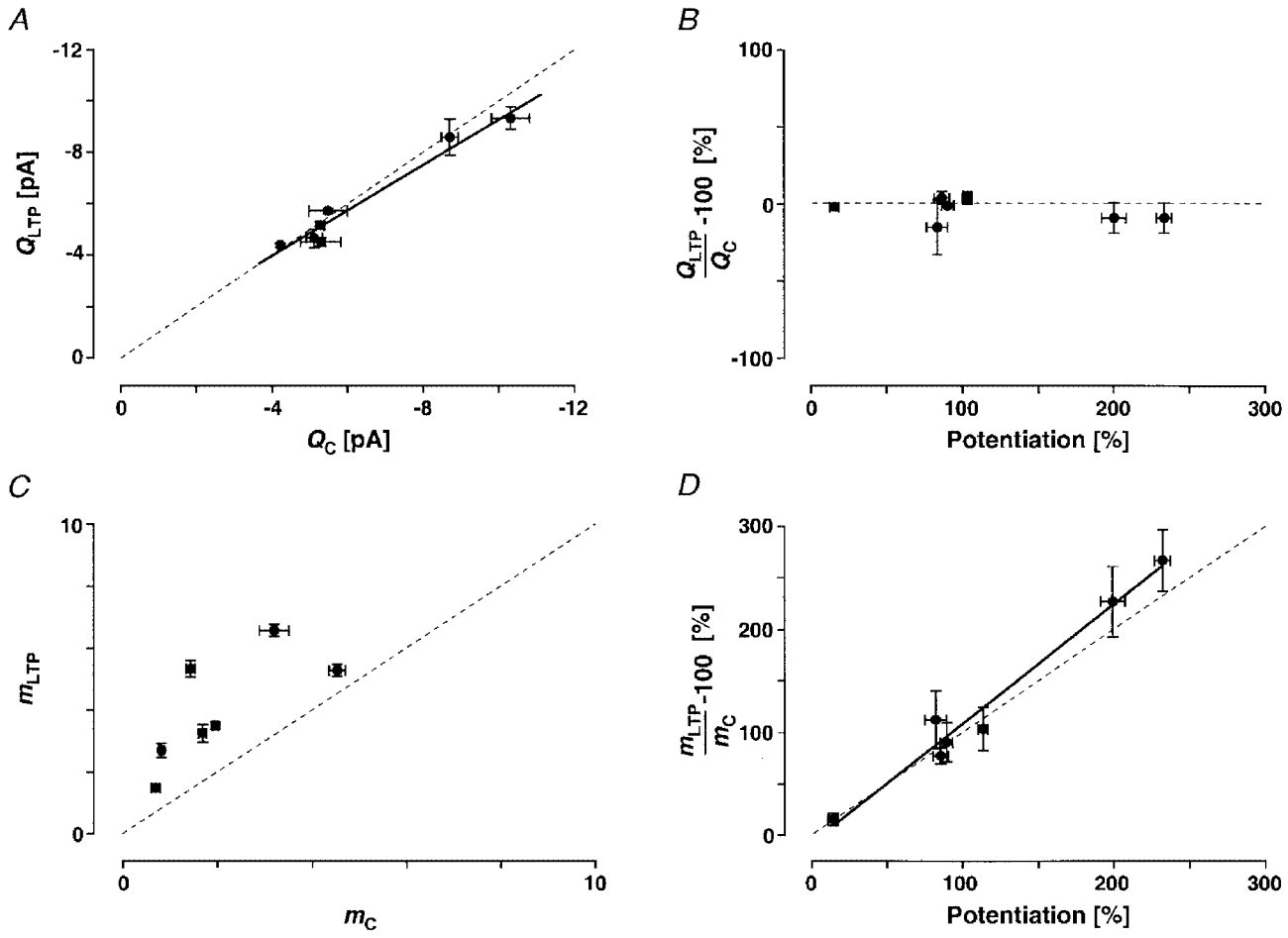

Figure 5

A, the quantal AMPA current before (Q_C) and after conditioning (Q_{LTP}), after correction for the attenuating effect of access resistance. The dashed line indicates equality, while the continuous line is a regression fit (Pearson $r = 0{\cdot}98$; $P < 0{\cdot}01$). *B*, the percentage change in quantal AMPA current plotted against the percentage change in the EPSC following conditioning, where zero indicates no change. The dashed line indicates no change in quantal size. Correlating the amount of potentiation with the change in quantal size, the level of significance (Pearson $r = -0{\cdot}39$; $P > 0{\cdot}1$) indicates that the regression line is not different from the dashed line. *C*, the quantal content before (m_c) and after conditioning (m_{LTP}). The dashed line indicates no change. *D*, the percentage change in quantal content, plotted against the percentage change in EPSC. Zero indicates no change. The dashed line indicates equality and the continuous line is the fit of a linear regression (Pearson $r = 0{\cdot}99$; $P < 0{\cdot}01$).

increase in quantal content normalised by the amount of potentiation was $71 \pm 39\%$ for NMDA-dependent LTP compared with $104 \pm 8\%$ in the present experiments ($n = 7$ in each case). While the difference in the normalised increase in quantal content is smaller for this restricted range of LTP, it is still significant ($P < 0{\cdot}05$). Similarly, the normalised percentage increase in quantal current for the same data was $20 \pm 30\%$ for NMDA-dependent LTP and $-4 \pm 8\%$ for the present experiments ($P = 0{\cdot}07$). Thus, there is a clear difference between the results obtained for NMDA-independent and NMDA-dependent LTP, regardless of the range of potentiation used in the comparison. Further evidence that the two data sets are different comes from comparing the regression fits to the percentage change in quantal content *versus* the percentage LTP, with and without APV present. Using a test for covariance (Snedecor & Cochran, 1989), the slopes of the two regression lines are significantly different ($P < 0{\cdot}01$). From all of the above comparisons, we conclude that NMDA-independent LTP is expressed as a change in quantal content, while NMDA-dependent LTP is expressed by changes in both quantal content and quantal current.

The increase in quantal content occurs because more sites become involved in transmission. An increase in release probabilities, or an increase in the number of active sites that contain functional groups of AMPA receptors, or both, could underlie the increase in quantal content. If the likelihood that transmission occurs at all synaptic sites (old and potentially new) is increased following conditioning, the probability of total failure of transmission will decrease. This was observed for 6/7 EPSCs (P_0, Table 1). If changes at all the synaptic sites are not homogeneous, with transmission more likely at some and less likely at others, it is possible to have an increased probability of transmission failure accompany an overall increase in the EPSC and the quantal content. This was observed for one EPSC (Cell 1, Table 1), as well as in previous results on NMDA-dependent LTP (Stricker *et al.* 1996*b*).

Is the NMDA current blocked in these experiments?

In the presence of 50 μM D,L-APV, 5–10 μM DNQX and depolarisation to −30 mV, all synaptic current was blocked (Fig. 3). This measurement was not done routinely, as it was clear from other reports that NMDA currents were completely blocked in CA1 pyramidal neurones (Hestrin *et al.* 1990) and interneurones (Sah *et al.* 1990) using 50 μM D,L-APV. Kullmann *et al.* (1992) ruled out residual NMDA currents in inducing NMDA-independent LTP, using 50 μM D-APV. Grover & Teyler (1994) systematically investigated the extent of NMDA blockade following single stimuli and tetani at different frequencies for different concentrations of

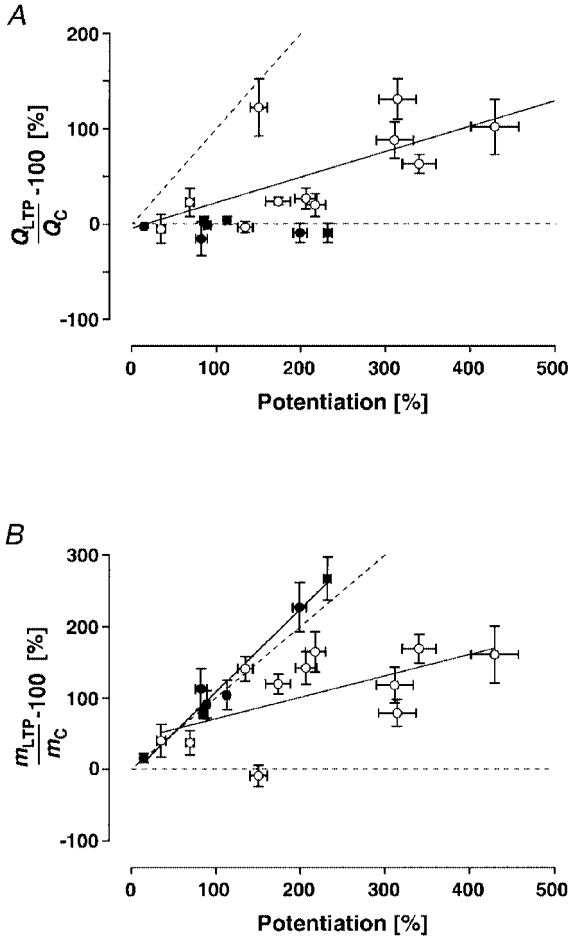

Figure 6

A, the results from Fig. 5*B* have been combined with the results from Fig. 3*B* in Stricker *et al.* (1996*b*). The filled circles correspond to the change in quantal current obtained in the present paper. The open circles correspond to the results obtained for NMDA-dependent LTP. Zero corresponds to no change in quantal current. The continuous line is the regression fit to the NMDA-dependent data set. The horizontal dashed line indicates no change in quantal size. The oblique dashed line is the line of equal change. *B*, the results from Fig. 5*D* have been combined with the results from Fig. 4*B* (Stricker *et al.* 1996*b*). The filled circles correspond to the changes in quantal content obtained in the present paper, while the open circles correspond to the results obtained for NMDA-dependent LTP. Zero corresponds to no change in quantal content. The two continuous lines are the regression fits to each set of data. The dashed lines are the line of equality (oblique) and no change in quantal content (horizontal).

D,L-APV and found that 50 μM D,L-APV reduced the NMDA EPSC to 8 $\pm$ 3 % of control. The extent of NMDA blockade during a tetanus is disputed (Grover & Teyler, 1994; Hanse & Gustafsson, 1995; Cummings *et al.* 1996). Higher concentrations of glutamate in the cleft would be expected under these conditions and as APV is a competitive antagonist, higher concentrations than those needed to block transmission evoked at low frequencies may be required.

As our results are completely different from those obtained using identical experimental conditions and analysis techniques, except for the presence of 50 μM D,L-APV, and as we have repeatedly demonstrated a complete blockade of NMDA currents evoked by a single stimulus at this concentration of APV, we assume that we have achieved an effective blockade of Ca^{2+} entry via the NMDA receptors.

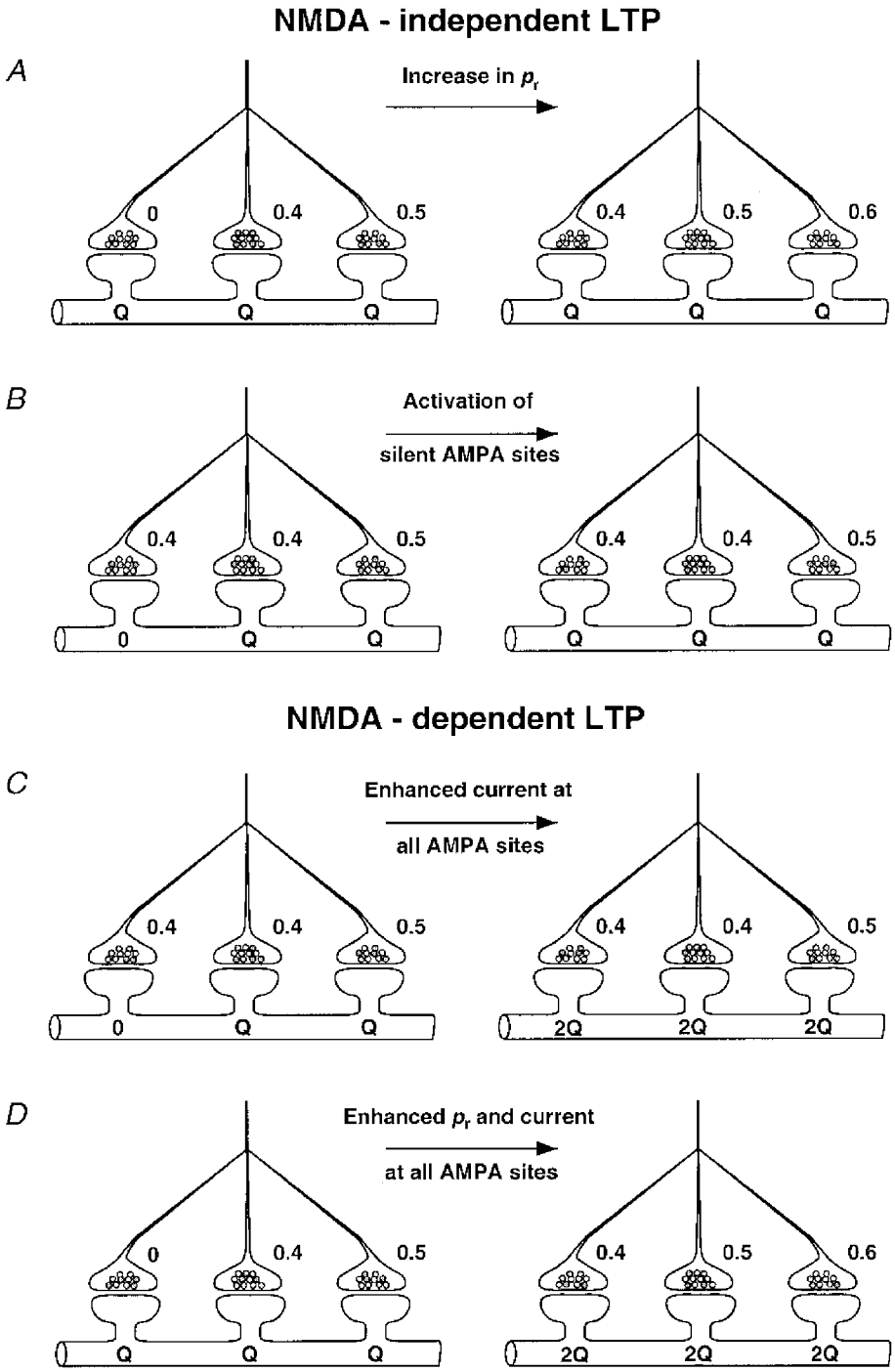

Figure 7. Schematic diagrams indicate different schemes for alterations in synaptic strength

The numbers adjacent to nerve terminals indicate release probabilities. The numbers under each spine indicate relative size of quantal AMPA currents. *A* and *B*, two alternative schemes for increasing quantal content while maintaining pre-existing quantal current in NMDA-independent LTP. *C* and *D*, two alternative schemes for increasing both quantal content and quantal current, while retaining quantised transmission after conditioning. p_r, probability of release.

Is the source of intracellular calcium important?

Chelation of postsynaptic calcium blocks the induction of NMDA-dependent LTP (Lynch *et al.* 1983) and NMDA-independent LTP (Teyler *et al.* 1994). Increases in cytoplasmic calcium occur during conditioning stimulation following calcium entry via NMDA receptors and voltage-dependent calcium channels (VDCC) (reviewed in Magee *et al.* 1998), and the release of calcium from internal stores by the action of IP_3, calcium or both of these substances (Berridge, 1993; Bliss & Collingridge, 1993; Sharp *et al.* 1993; Emptage *et al.* 1999; but see Yuste *et al.* 1999). It is possible that cytoplasmic calcium originating from these different sources will have differential effects on downstream signalling outcomes (Teyler *et al.* 1994). This could occur through compartmentalization of calcium from different sources, or through different calcium concentration thresholds for different second messenger cascades. For example, calcium entering via NMDA receptors or VDCCs induced two different forms of TEA-LTP in CA1 neurones (Huber *et al.* 1995). Transient enhancement of EPSCs induced by voltage pulsing in the presence of NMDA antagonists is not occluded by LTP induced either by tetanic stimulation (Chen *et al.* 1998) or by low-frequency stimulation combined with maintained depolarisation (Kullmann *et al.* 1992), when NMDA antagonists are not present. This occlusion, and other differences between these two forms of potentiation, led Chen *et al.* (1998) to propose that the two forms of potentiation were initiated from separate sources of calcium. Tetanically induced NMDA-dependent LTP occluded tetanically induced NMDA-independent LTP, but no occlusion occurred when the sequence was reversed. This result, and the differential action of the broad spectrum protein kinase inhibitor H-7 on the induction of both these forms of LTP, led Grover & Teyler (1995) to suggest that the signalling pathways for these two forms of LTP were either independent, or had a common component.

Our results suggest a linkage between calcium entering via NMDA receptors and maintained enhancement of AMPA currents. It is known that calcium–calmodulin-dependent kinase II (CaMKII) is associated with the NMDA receptor (Leonard *et al.* 1999), that AMPA channels are phosphorylated by CaMKII (Barria *et al.* 1997), that this phosphorylation increases AMPA channel conductance (Derkach *et al.* 1999), and that increased AMPA current following induction has been attributed to increased AMPA channel conductance (Benke *et al.* 1998), as well as the appearance of new patches of AMPA channels (Shirke & Malinow, 1997). This evidence is consistent with the idea that calcium entering through the NMDA receptors is specifically used to enhance AMPA currents rather than the notion that it combines with other sources of calcium to reach a threshold for this signalling pathway.

AMPA currents can be enhanced, however, in the absence of NMDA channel activation by nerve stimulation (Wyllie *et al.* 1994). Similarly, these authors demonstrated that the amplitude and frequency of AMPA mEPSCs can be transiently increased following a depolarising voltage pulse protocol in 4 mM Ca^{2+} without direct activation of NMDA receptors. The increase in AMPA current was shown to be blocked by the CaMKII inhibitor KN62 (Wyllie & Nicoll, 1994) indicating that this kinase was responsible for the enhancement of the AMPA current. Yet this transient increase in AMPA current was not occluded by NMDA-dependent LTP, where AMPA currents were enhanced in a maintained fashion (Kullmann *et al.* 1992). Our results suggest that the maintained increase in AMPA currents, which is a characteristic of normal LTP, is triggered by calcium entry through NMDA channels, which presumably activates CaMKII. How can these apparently conflicting results be reconciled? One possibility is that if the conditioning protocol ensures a very large calcium influx, such as in Wyllie *et al.* (1994), calcium from both sources can access the CaMKII pathway. This is consistent with the threshold concept for calcium access to this signalling pathway, but it would not explain why one source of calcium led to a transient enhancement of AMPA channels, while the other source resulted in a maintained enhancement. Another possibility is that KN62 is not a highly specific inhibitor of CaMKII, as the results of Marley & Thomson (1996) may indicate. There are other signalling pathways known to affect AMPA channels, such as those involving the tyrosine kinase *src* (Lu *et al.* 1998), cyclic AMP-dependent kinase (Greengard *et al.* 1991) and the calcium-dependent protease calpain (Gellerman *et al.* 1997). If KN62 can inhibit any of these kinases, the transient enhancement in AMPA channels may not be due to CaMKII. We cannot resolve this issue with our data.

Alterations in synaptic strength following LTP induction

The observed increase in quantal content could be a result of an increased probability of release at the synapses involved in transmission before conditioning, including synapses which had very low probabilities and were effectively silent. This scheme is illustrated in Fig. 7*A* and it requires a retrograde signal. The increased quantal content could also result from an increase in the number of sites at which transmission occurs as a result of activating functional groups of AMPA receptors at these new sites (Liao *et al.* 1995). This scheme is illustrated in Fig. 7*B*, and it requires the modulation of AMPA currents to occur only at postsynaptic sites where there were no functional AMPA channels before conditioning. It is consistent with the conclusions reached by Grover (1998) on the expression of NMDA-independent LTP. A combination of both mechanisms (Fig. 7*A* and *B*) would also provide an increase in quantal content. We are unable to calculate release probabilities before and after conditioning, as the data cannot be explained by conventional models of transmitter release (binomial or Poisson). That means we cannot distinguish between the alternative explanations above for increased quantal content. However, our results allow us to impose constraints on changes that must occur at synapses

following conditioning when either functional or non-functional NMDA receptors are present. These constraints must satisfy the observation that quantal AMPA current is the same before and after the induction of NMDA-independent LTP, while following the induction of NMDA-dependent LTP the quantal current is increased (Stricker *et al.* 1996*b*).

Two alternative schemes that can explain the previously published results of quantal analysis of NMDA-dependent LTP (Stricker *et al.* 1996*b*) are shown in Fig. 7*C* and *D*. Quantisation is preserved with an increased quantal current and quantal content in the scheme illustrated in Fig. 7*C*, which requires AMPA currents at both previously functional and non-functional sites to be activated, but by different amounts so as to maintain quantisation. The alternative illustrated in Fig. 7*D* is a mixture of pre- and postsynaptic changes. It requires an increase in release probabilities, and all AMPA currents to increase by the same amount. The schemes illustrated in Fig. 7*A* and *D* are less complicated in the sense that they do not require different increases in AMPA currents at previously silent and functional synapses. The quantal AMPA current is either not changed at all synapses, or it is changed by the same amount at all synapses. Our results suggest that this change in the AMPA current at previously functional sites is initiated by the Ca^{2+} influx through the NMDA receptors. Calcium increases from non-NMDA sources can be used to initiate increases in quantal content; either by activation of new AMPA sites (Fig. 7*B*), increases in release probabilities (Fig. 7*A*) or a combination of both. This discussion assumes that NMDA-independent LTP is a subset of NMDA-dependent LTP as is suggested by the observation that the dependent form occludes the independent form, but not vice versa (Grover & Teyler, 1995). It remains possible that the NMDA-independent LTP examined here requires an entirely different signalling cascade to alter quantal content from the one used in NMDA-dependent LTP.

The literature is awash with competing claims for pre- and postsynaptic changes associated with LTP. Some of the confusion almost certainly arises because of the different experimental conditions and protocols under which LTP is induced and maintained (Larkman & Jack, 1995). Animal age, temperature of preparation, external calcium concentration, electrode solutions and type of preparation (slice, culture and *in vivo*) are all confounding variables. The result of these experiments does not alleviate the pre-*versus* postsynaptic issue, but they do provide some insight into how calcium may be used during LTP induction. When NMDA channels are blocked, the increase in cytosolic calcium is either below threshold for enhancing the AMPA current at synapses previously involved in transmission, or it is unavailable to the signalling pathway used for this enhancement. This calcium either initiates increases in release probabilities or unmasks AMPA receptors at previously non-functional AMPA sites, or it triggers both of these changes. When additional calcium enters the spine via NMDA receptors, the signalling pathway for enhancing AMPA currents at previously functional sites is activated, either because the required calcium threshold is reached or because calcium through NMDA channels specifically activates this signalling pathway.

Barria, A., Muller, D., Derkach, V. A., Griffith, L. C. & Soderling, T. R. (1997). Regulatory phosphorylation of AMPA-type glutamate receptors by CaM-KII during long-term potentiation. *Science* **276**, 2042–2045.

Benke, T. A., Lüthi, A., Isaac, J. T. R. & Collingridge, G. L. (1998). Modulation of AMPA receptor unitary conductance by synaptic activity. *Nature* **393**, 793–797.

Berridge, M. J. (1993). Inositol trisphosphate and calcium signalling. *Nature* **361**, 315–325.

Bliss, T. V. P. & Collingridge, G. L. (1993). A synaptic model of memory: long-term potentiation in the hippocampus. *Nature* **361**, 31–39.

Chen, H.-X., Hanse, E., Pananceau, M. & Gustafsson, B. (1998). Distinct expressions for synaptic potentiation induced by calcium through voltage-gated calcium and *N*-methyl-D-aspartate receptor channels in the hippocampal CA1 region. *Neuroscience* **86**, 415–422.

Collingridge, G. L., Kehl, S. J. & McLennan, H. (1983). The antagonism of amino acid-induced excitations of rat hippocampal CA1 neurones *in vitro*. *Journal of Physiology* **334**, 19–31.

Cummings, J. A., Mulkey, R. M., Nicoll, R. A. & Malenka, R. C. (1996). Ca^{2+} signalling requirements for long-term depression in the hippocampus. *Neuron* **16**, 825–833.

Derkach, V. A., Barria, A. & Soderling, T. R. (1999). Ca^{2+}/calmodulin-kinase II enhances channel conductance of α-amino-3-hydroxy-5-methyl-4-isoxazolepropionate type glutamate receptors. *Proceedings of the National Academy of Sciences of the USA* **96**, 3269–3274.

Emptage, N. J., Bliss, T. V. P. & Fine, A. (1999). Single synaptic events evoke NMDA receptor-mediated release of calcium from internal stores in hippocampal dendritic spines. *Neuron* **22**, 115–124.

Gellerman, D. M., Bi, X. & Baudry, M. (1997). NMDA receptor-mediated regulation of AMPA receptor properties in organotypic hippocampal slice cultures. *Journal of Neurochemistry* **69**, 131–136.

Greengard, P., Jen, J., Nairn, A. C. & Stevens, C. F. (1991). Enhancement of the glutamate response by cAMP-dependent protein kinase in hippocampal neurons. *Science* **253**, 1135–1138.

Grover, L. M. (1998). Evidence for postsynaptic induction and expression of NMDA receptor independent LTP. *Journal of Neurophysiology* **79**, 1167–1182.

Grover, L. M. & Teyler, T. J. (1990*a*). Effects of extracellular potassium concentration and postsynaptic membrane potential on calcium-induced potentiation in area CA1 of rat hippocampus. *Brain Research* **506**, 53–61.

Grover, L. M. & Teyler, T. J. (1990*b*). Two components of long-term potentiation induced by different patterns of afferent activation. *Nature* **347**, 477–479.

Grover, L. M. & Teyler, T. J. (1994). Activation of NMDA receptors in hippocampal area CA1 by low and high frequency orthodromic stimulation and their contribution to induction of long-term potentiation. *Synapse* **16**, 66–75.

Grover, L. M. & Teyler, T. J. (1995). Different mechanisms may be required for maintenance of NMDA receptor-dependent and independent forms of long-term potentiation. *Synapse* **19**, 121–133.

Hanse, E. & Gustafsson, B. (1995). Long-term potentiation in the hippocampal CA1 region in the presence of *N*-methyl-D-aspartate receptor antagonists. *Neuroscience* **67**, 531–539.

Hestrin, S., Nicoll, R. A., Perkel, D. J. & Sah, P. (1990). Analysis of excitatory synaptic action in pyramidal cells using whole-cell recording from rat hippocampal slices. *Journal of Physiology* **422**, 203–225.

Huber, K. M., Mauk, M. D. & Kelly, P. T. (1995). Distinct LTP induction mechanisms: Contribution of NMDA receptors and voltage-dependent calcium channels. *Journal of Neurophysiology* **73**, 270–279.

Kullmann, D. M., Perkel, D. J., Manabe, T. & Nicoll, R. A. (1992). Ca^{2+} entry via postsynaptic voltage-sensitive Ca^{2+} channels can transiently potentiate excitatory synaptic transmission in the hippocampus. *Neuron* **9**, 1175–1183.

Larkman, A. U. & Jack, J. J. B. (1995). Synaptic plasticity: Hippocampal LTP. *Current Opinion in Neurobiology* **5**, 324–334.

Leonard, A. S., Lim, I. A., Hemsworth, D. E., Horne, M. C. & Hell, J. W. (1999). Calcium/calmodulin-dependent protein kinase II is associated with the *N*-methyl-D-aspartate receptor. *Proceedings of the National Academy of Sciences of the USA* **96**, 3239–3244.

Liao, D., Hessler, N. A. & Malinow, R. (1995). Activation of postsynaptically silent synapses during pairing-induced LTP in CA1 region of hippocampal slice. *Nature*, **375**, 400–404.

Lu, Y.-M., Roder, J. C., Davidow, J. & Salter, M. W. (1998). *Src* activation in the induction of long-term potentiation in CA1 hippocampal neurons. *Science* **279**, 1363–1367.

Lynch, G. S., Larson, J., Kelso, S. R., Barrionuevo, G. & Schottler, F. (1983). Intracellular injections of EGTA block induction of hippocampal long-term potentiation. *Nature* **305**, 719–721.

Magee, J. C., Hoffman, D. A., Colbert, C. M. & Johnston, D. (1998). Electrical and calcium signaling in dendrites of hippocampal pyramidal neurons. *Annual Review of Physiology* **60**, 327–346.

Marley, P. D. & Thomson, K. A. (1996). The Ca^{2+}/calmodulin-dependent protein kinase II inhibitors KN62 and KN93, and their inactive analogues KN04 and KN92, inhibit nicotinic activation of tyrosine hydroxylase in bovine chromaffin cells. *Biochemical and Biophysical Research Communications* **221**, 15–18.

Sah, P., Hestrin, S. & Nicoll, R. A. (1990). Properties of excitatory postsynaptic currents recorded *in vitro* from rat hippocampal interneurones. *Journal of Physiology* **430**, 605–616.

Sharp, A. H., McPherson, P. S., Dawson, T. M., Aoki, C., Campbell, K. P. & Snyder, S. H. (1993). Differential immunohistochemical localization of inositol 1,4,5-trisphosphate- and ryanodine-sensitive Ca^{2+} release channels in rat brain. *Journal of Neuroscience* **13**, 3051–3063.

Shirke, A. M. & Malinow, R. (1997). Mechanisms of potentiation by calcium-calmodulin kinase II of postsynaptic sensitivity in rat hippocampal CA1 neurons. *Journal of Neurophysiology* **78**, 2682–2692.

Snedecor, G. W. & Cochran, W. G. (1989). *Statistical Methods*. Iowa State University Press, Ames.

Stricker, C., Daley, D. & Redman, S. J. (1994). Statistical analysis of synaptic transmission: Model discrimination and confidence limits. *Biophysical Journal* **67**, 532–547.

Stricker, C., Field, A. C. & Redman, S. J. (1996*a*). Statistical analysis of amplitude fluctuations in EPSCs evoked in rat CA1 pyramidal neurones *in vitro*. *Journal of Physiology* **490**, 419–441.

Stricker, C., Field, A. C. & Redman, S. J. (1996*b*). Changes in quantal parameters of EPSCs in rat CA1 neurones *in vitro* after the induction of long-term potentiation. *Journal of Physiology* **490**, 443–454.

Stricker, C. & Redman, S. J. (1994). Statistical models of synaptic transmission evaluated using the expectation-maximization algorithm. *Biophysical Journal* **67**, 656–670.

Teyler, T. J., Çavus, I., Coussens, C. M., DiScenna, P., Grover, L. M., Lee, Y. P. & Little, Z. (1994). Multideterminant role of calcium in hippocampal synaptic plasticity. *Hippocampus* **4**, 623–634.

Wyllie, D. J. A., Manabe, T. & Nicoll, R. A. (1994). A rise in postsynaptic Ca^{2+} potentiates miniature excitatory postsynaptic currents and AMPA responses in hippocampal neurons. *Neuron* **12**, 127–138.

Wyllie, D. J. A. & Nicoll, R. A. (1994). A role for protein kinases and phosphatases in the Ca^{2+}-induced enhancement of hippocampal AMPA receptor-mediated synaptic responses. *Neuron* **13**, 635–643.

Yuste, R., Majewska, A., Cash, S. S. & Denk, W. (1999). Mechanisms of calcium influx into hippocampal spines: Heterogeneity among spines, coincidence detection by NMDA receptors, and optical quantal analysis. *Journal of Neuroscience* **19**, 1976–1987.

Acknowledgements

The authors are grateful for the critical comments provided by Professor Julian Jack and Dr John Bekkers on an earlier draft of this paper. This work was in part supported by the following grants to C.S.: Swiss National Science Foundation (5002-242787), Bonizzi-Theler Foundation and Jubiläumsstiftung der Schweizerischen Mobiliar Versicherungsanstalt.

Corresponding author

S. J. Redman: Division of Neuroscience, John Curtin School of Medical Research, Australian National University, GPO Box 334, Canberra, ACT 0200, Australia.

Email: steve.redman@anu.edu.au